Check for updates

Geophysical Research Letters

RESEARCH LETTER
10.1029/2023GL107209

The Impact of the South Atlantic Anomaly on the Aurora System

Z.-Y. Liu[1], Q.-G. Zong[1,2], L. Li[1], Z.-J. Feng[1], Y.-X. Sun[1], X.-Q. Yu[1], Y.-F. Wang[1], J.-J. Liu[3], and Z.-J. Hu[3]

[1]Institute of Space Physics and Applied Technology, Peking University, Beijing, China, [2]State Key Laboratory of Lunar and Planetary Sciences, Macau University of Science and Technology, Macau, China, [3]Polar Research Institute of China, Shanghai, China

Key Points:

- The effects of the South Atlantic Anomaly (SAA) on the terrestrial aurora system are examined using multiple instruments
- Observations reveal a substantial weakening of auroral magnetic fluctuations and auroral intensity in the SAA longitude sector
- The results indicate considering magnetic anomalies like the SAA is essential for comprehensively understanding planetary aurora systems

Correspondence to:
Q.-G. Zong,
qgzong@pku.edu.cn

Citation:
Liu, Z.-Y., Zong, Q.-G., Li, L., Feng, Z.-J., Sun, Y.-X., Yu, X.-Q., et al. (2024). The impact of the south Atlantic anomaly on the aurora system. *Geophysical Research Letters*, *51*, e2023GL107209. https://doi.org/10.1029/2023GL107209

Received 16 NOV 2023
Accepted 11 JAN 2024

© 2024. The Authors.
This is an open access article under the terms of the Creative Commons Attribution-NonCommercial-NoDerivs License, which permits use and distribution in any medium, provided the original work is properly cited, the use is non-commercial and no modifications or adaptations are made.

Abstract The South Atlantic Anomaly (SAA) refers to a region where the strength of the magnetic field is notably weaker compared to a dipole field. While previous studies have primarily focused on its effects on the inner radiation belt, this study investigates its impact on the aurora system. By analyzing 2 years' worth of data obtained by the Fengyun-3E/ACMag instrument, we discover that magnetic fluctuations within the auroral oval are significantly weaker in the longitude sector corresponding to the SAA, as compared to those outside this area. This characteristic remains permanent and independent of seasons and geomagnetic activities. Additional investigation using Defense Meteorological Satellite Program/Special Sensor Ultraviolet Spectrographic Imager (DMSP/SSUSI) observations reveals a similar phenomenon in the auroral intensity. Therefore, our results demonstrate that the SAA substantially weakens the aurora system, shedding new light on the effects of magnetic anomalies on planetary auroras and magnetosphere-ionosphere-thermosphere coupling.

Plain Language Summary The South Atlantic Anomaly (SAA) is a unique location on Earth where the magnetic field is weaker than normal. This region has drawn a lot of attention because its weakened magnetic field brings the inner Van Allen radiation belt unusually close to the Earth's surface, which poses a threat to satellites passing through it. Here, we uncovered another interesting aspect of the SAA: its impact on the aurora system. To investigate this, we first examined 2 years' worth of data from the ACMag instruments on the Fengyun-3E satellite, which orbits the Earth at an altitude of 836 km in a dawn-dusk, Sun-synchronous orbit. Our findings reveal that the magnetic fluctuations within the southern auroral oval are significantly weaker in the region that aligns with the SAA. This weakening effect is consistently present, regardless of the season or the level of geomagnetic activity. To reinforce our results, we also analyzed auroral intensity from the Special Sensor Ultraviolet Spectrographic Imager (SSUSI) instrument on the Defense Meteorological Satellite Program (DMSP) satellite, and it corroborated the same weakening trend in this data set. In conclusion, our observations demonstrate that the SAA has a substantial impact on weakening the aurora system. This discovery deepens our understanding of how magnetic anomalies can influence planetary auroras.

1. Introduction

The term "magnetosphere" inherently implies the crucial presence of magnetic fields within planetary magnetospheres. These fields can be regarded as magnetospheres' "skeleton," constricting the physical shape and energetic dynamics of magnetospheres. Within a specific magnetosphere, the magnetic fields can be further categorized into various subcomponents, each with its distinct origin. An essential subcomponent to consider is the internal magnetic field generated by currents within planets' body. In the case of Earth, this field is often approximated as a geocentric dipole field in most regions of the magnetosphere. However, in certain areas, non-dipole components become significant. The South Atlantic Anomaly (SAA) serves as a prominent example.

The SAA refers to a region where the strength of the magnetic fields is notably weaker compared to the dipole field. At present, this region is located over northern South America and the South Atlantic (Badhwar, 1997; Finlay et al., 2020). The SAA is famous for its impact on the inner Van Allen belt, as the diminished magnetic fields allow the belt to come closest Earth's surface within this area (Ginet et al., 2014; Gledhill, 1976; Heirtzler, 2002; Roederer & Zhang, 2016). Consequently, this proximity results in a substantial increase in energetic particle fluxes (e.g., Ginet et al., 2014), which poses a threat to satellites passing through it (e.g., Gledhill, 1976; Heirtzler, 2002; Underwood, 2003).

19448007, 2024, 3, Downloaded from https://agupubs.onlinelibrary.wiley.com/doi/10.1029/2023GL107209 by Cochrane Iceland, Wiley Online Library on [27/01/2025]. See the Terms and Conditions (https://onlinelibrary.wiley.com/terms-and-conditions) on Wiley Online Library for rules of use; OA articles are governed by the applicable Creative Commons License

Although previous studies primarily focus on the effects of the SAA at the mid-latitudes (~40°), where the inner belt is situated, the SAA itself extends continuously to higher latitudes, as illustrated by, for example, Badhwar (1997), Finlay et al. (2020), and observations presented below. This extension raises the potential for affecting various components of the magnetosphere beyond the inner belt. The main objective of this paper is to investigate a specific aspect of this phenomenon: the influence of the SAA on the aurora system. The aurora serves as the imaging of magnetospheric activities (Paschmann et al., 2003). Consequently, any possible aberrations caused by the SAA have the potential to lead to misinterpretations when analyzing auroral observations and attempting to comprehend magnetospheric processes based on such observations. Moreover, knowledge of the influence of the SAA on Earth's aurora system yields general insight into how magnetic anomalies affects planetary aurora and the broader concept of magnetosphere-ionosphere-thermosphere (MIT) coupling. This research also sheds light on the auroral dynamics and MIT coupling on other planets where non-dipole components hold more significance compared to Earth, such as Jupiter (e.g., Connerney et al., 2022; Grodent et al., 2008) and Mars (e.g., Connerney et al., 2001; Langlais et al., 2004).

The investigation presented here is primarily based on the high-frequency magnetic fields measured by the AC Vector Magnetometer (ACMag) instrument (Liu et al., 2023; Yu, Huang, et al., 2023) onboard the FengYun-3E (FY3E) satellite. The next section will systematically present the observations and demonstrate that the magnetic fluctuations within the auroral oval are notably weaker within the longitude range influenced by the SAA, in comparison to other longitudes. To reinforce this observation and further elucidate the impact of the SAA on the aurora system, in Section 3 we also examine Defense Meteorological Satellite Program/Special Sensor Ultraviolet Spectrographic Imager (DMSP/SSUSI; Paxton & Meng, 1999; Paxton et al., 2002) observations of auroral intensity, which show similar results to the ACMag instrument. Subsequently, we discuss and summarize our main findings in Sections 4 and 5, respectively.

2. Fengyun-3E/ACMag Observations

2.1. Auroral Magnetic Fluctuations Observed by ACMag

The FY3E satellite was launched in July of 2021 and was inserted into a dawn-dusk Sun-synchronous orbit with the following parameters: altitude ~836 km, inclination~99° (thus there is a small latitude range near the poles that the satellite does not cover), period~102 min and the period of orbital regression~5.5 days. Various space weather-relevant instruments are onboard this satellite. Here, we primarily analyze the data obtained by the ACMag instrument developed by the Peking University instrument development team. This instrument is designed to measure the three-dimensional magnetic field within the frequency range 0.05–25 Hz (Yu, Huang, et al., 2023).

Figures 1b–1e shows typical ACMag observations in the south hemisphere, whereas Figure 1a gives the deviations of the azimuthal component (B_a) of the DC magnetic fields from the International Geomagnetic Reference Field model measured by the FY3E/DC Vector Magnetometer (DCMag) instrument (Yu, Li, et al., 2023) during the same time interval. Deviation of B_a from the baseline is observed near the magnetic latitude (MLAT) ~ −70° in both the dawn and dusk sectors, indicating the passing of the satellite through the Birkeland field-aligned current system as well as the approximately co-located aurora oval (e.g., Iijima & Potemra, 1978; Lühr et al., 2015]. Within these regions, clear wavy signals appear in the magnetic fields detected by ACMag. The nature of these signals is still under extensive discussion; they may represent plasma waves Alfvén waves in most cases) (e.g., Lühr et al., 2015; Pakhotin et al., 2018, 2020), quasi-static small-scale FACs (i.e., moving charged particles) (e.g., Consolini et al., 2020; Golovchanskaya et al., 2006), or any combination of the two. In this paper, we do not intervene in this debate, as it is difficult in practice to separate out waves from small-scale FACs (e.g., Trenchi et al., 2020) and we cannot provide any conclusive evidence with the current single-spacecraft observations. Instead, we simply refer to them as auroral magnetic fluctuations and note they are closely related with the aurora, no matter their specific physical nature.

Figure 1e shows the dynamical spectra of the magnetic fields shown in Figures 1b and 1c. Here, the color codes indicate the total power, defined as $B_w^2 = B_x^2 + B_y^2 + B_z^2$, where B_i^2 with $i = x, y, z$ represents the power in the corresponding direction derived from a windowed fast Fourier transformation with a 20-s window. The two white vertical stripes result from data gaps during the corresponding time intervals. Additionally, the horizontal stripes extending continuously from the left to the right represent noises caused by the satellite or other instruments

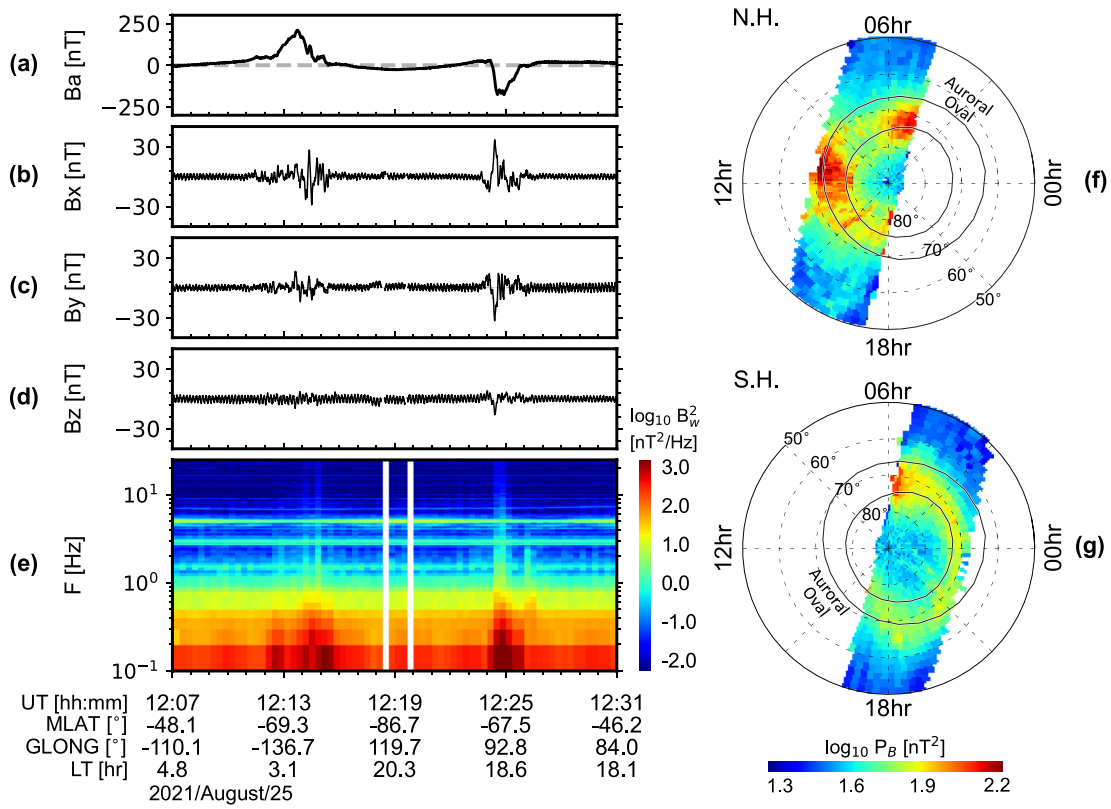

Figure 1. FengYun-3E/ACMag observations of auroral magnetic fluctuations (a–e) Example of ACMag observations in the southern hemisphere on 25 August 2021. (a) Deviations of the azimuthal component of the DC magnetic fields (measured by the DCMag instrument) from the International Geomagnetic Reference Field magnetic field model (b–c) AC magnetic fields in the geographic coordinates measured by the ACMag instrument. (e) Dynamical spectra of the AC magnetic fields shown in panels (b–c), with the color codes representing the total power defined in the main text. (f and g) Magnetic local time-magnetic latitude distributions of integrated power (0.1–10 Hz) in the northern and southern hemispheres, respectively, generated from the ACMag instrument data during 10 July 2021, to 24 April 2023. The solid curves represent the average location of the auroral oval given by Hu et al. (2017).

onboard. Fortunately, these noises have minimal impact on our analysis for two reasons: First, they exhibit minimal temporal variation, and second, their contribution to the integrated power focused on below is significantly lower than that of the actual signals. In Figure 1e, it becomes evident that the dynamical spectra display enhancement within the entire shown frequency range within the auroral oval.

In this study, we do not consider the detailed shape of these spectra, even though they may also be influenced by the SAA. Instead, our focus is solely on the integrated power defined as $P_B = \int_{f_l}^{f_u} B_w^2(f)df$, where $f_l = 0.1$ Hz is set so to avoid the influence of satellite motion and $f_u = 10$ Hz is approximately the Nyquist frequency of ACMag (Liu et al., 2023). Figures 1f and 1g present the magnetic local time (MLT)-MLAT distributions of P_B in the northern and southern hemispheres, respectively. The values shown in these figures are generated from ACMag observations obtained from 10 July 2021, to 24 April 2023, and they represent the median values at each position. Notably, P_B in both hemispheres peaks within the statistical auroral oval marked by the black curves (Hu et al., 2017), aligning with previous observations (Keiling et al., 2003, 2019; Liu et al., 2023).

When creating Figures 1f and 1g, we combine data from all longitudes together, as is commonly done in the literature (Keiling et al., 2003, 2019; Knipp et al., 2021; Liu et al., 2023; Pakhotin et al., 2021). However, we will demonstrate in the following that this procedure may not be applied to the southern hemisphere, where P_B shows significant dependence on longitudes, although it may be safely applied to the northern hemisphere.

2.2. Weakness of Auroral Magnetic Fluctuations at the SAA

In this subsection, we turn to the geographic distributions of P_B. In what follows, data from all MLT are combined together. Nevertheless, as indicated by Figures 1f and 1g, the data for the northern and southern hemispheres are

19448007, 2024, 3, Downloaded from https://agupubs.onlinelibrary.wiley.com/doi/10.1029/2023GL107209 by Cochrane Iceland, Wiley Online Library on [27/01/2025]. See the Terms and Conditions (https://onlinelibrary.wiley.com/terms-and-conditions) on Wiley Online Library for rules of use; OA articles are governed by the applicable Creative Commons License

19448007, 2024, 3, Downloaded from https://agupubs.onlinelibrary.wiley.com/doi/10.1029/2023GL107209 by Cochrane Iceland, Wiley Online Library on [27/01/2025]. See the Terms and Conditions (https://onlinelibrary.wiley.com/terms-and-conditions) on Wiley Online Library for rules of use; OA articles are governed by the applicable Creative Commons License

obtained in the dayside and nightside local times, respectively, due to the orbit geometry of FY3E. Therefore, when considering a single hemisphere, the potential bias arising from MLT-dependence (primarily the day-night contrast) should be weak.

Figure 2a presents the main result of this paper. First, the thin gray curves depict the coastlines, while the blue-coded curves represent the contours of the strength of the background geomagnetic fields (B) observed by DCMag, with darker shades of blue indicating smaller values (the specific values are given by the attached figures). These blue-coded curves demonstrate that B is weaker over the northern South America and the South Atlantic, which corresponds to the SAA (Badhwar, 1997; Finlay et al., 2020). Besides, they also show the region of weaker B than the surroundings continuously extends to higher latitudes and connects with the auroral latitudes at $\sim -90° <$ longitude $< 90°$, confirming our earlier statements in the introduction section.

The color codes presented in Figure 2a give the geographic distributions of P_B during the period from 10 July 2021, to 24 April 2023, with the median value at each position represented. Two ribbons of enhanced P_B are observed at high latitudes, representing the magnetic fluctuations within the auroral oval discussed above. These ribbons closely follow the iso-magnetic latitude lines. To illustrate this point, the four black curves, from top to bottom, represent the 85°, 71°, −63° and −77° latitudes in the Altitude-Adjusted Corrected Geomagnetic coordinates (Shepherd, 2014). Evidently, these curves accurately capture the regions of large P_B (The differences in latitudes between the northern and southern hemispheres reflect the fact that data in different hemispheres are obtained at different local times; see Figures 1f and 1g.)

A careful examination of Figure 2a reveals that P_B in the southern auroral oval is significantly smaller within the longitude range from $\sim -$ 90°–90°, compared to other longitudes (indicated by yellow colors v.s. red colors). To quantify this feature, we extract the peak values of P_B in the latitude range bounded by the two black curves at each longitude and show them in Figure 2c as a black curve after normalizing them with their maximum value. It is evident that the normalized P_B exhibits a significant decrease within $\sim -90° <$ longitude $< 90°$, with the amplitude of decrease exceeding 55%. Interestingly, the region of lower P_B coincides with the region of weaker B corresponding to the SAA. This observation can be directly seen from Figure 2a or by comparing the black curve with the gray curve presented in Figure 2c, where the latter represents B within the southern auroral oval extracted and processed in the same way as P_B.

Furthermore, it is noted that the reduction in power at the SAA longitudes is not limited to the total magnetic field but also exists in its individual components. Figures 2d and 2e illustrate the geographic distributions of the integrated power for the azimuthal and meridional components of the magnetic fluctuations measured by ACMag, respectively, in the southern hemisphere. Here, the azimuthal direction is defined as perpendicular to both the background magnetic fields and the magnetic meridional plane, while the meridional direction is defined as lying within the magnetic meridional plane and perpendicular to the background magnetic fields, where here the background magnetic fields are obtained by applying a second-order, 100-s window Savitsky-Golay filter to the DCMag data (Billett et al., 2022). It is evident that both the two components experience a notable decrease in the longitude range of $\sim -90°$–90°, indicating the presence of the SAA effect.

In contrast, P_B in the northern auroral oval exhibits a relatively homogenous distribution across longitudes (Figure 2a). This can be seen from Figure 2b as well, which is similar to Figure 2c except showing the northern hemisphere case. One can see that, while some variations are also present in P_B, the amplitude is significantly smaller (<25%) compared to the case of southern hemisphere. Likewise, B in the northern auroral oval remains relatively constant as well.

Therefore, from Figure 2, we conclude that the auroral magnetic fluctuations are weaker in the SAA longitude sector as compared to those outside.

2.3. Observations Under Different Conditions

Previous studies have found that the magnetic fluctuations within the auroral oval can be influenced by various parameters, particularly seasons (e.g., Erlandson & Zanetti, 1998) and the level of geomagnetic activity (e.g., Keiling et al., 2019; Liu et al., 2023). Therefore, in this subsection, we investigate the phenomenon identified above under diverse conditions, to demonstrate its permanence as a feature (Only the southern hemisphere is shown from now on. However, we have also examined the northern hemisphere and found the corresponding distributions are homogeneous with respect to longitudes.)

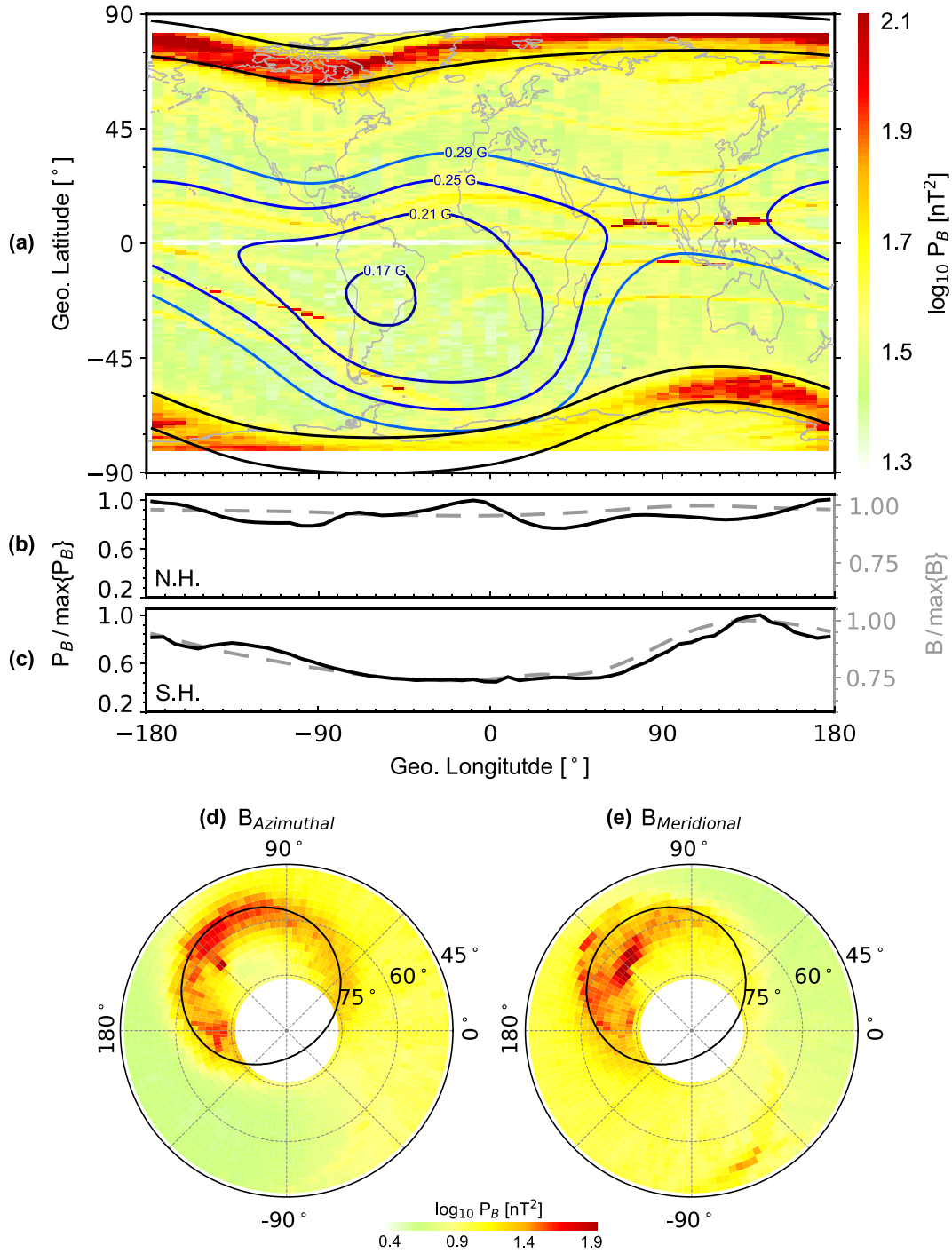

Figure 2. Geographic distributions of integrated power (0.1–10 Hz) in auroral magnetic fluctuations measured by the ACMag instrument from 10 July 2021 to 24 April 2023. (a) Geographic distributions of the integrated power (color codes). The blue curves represent contours of geomagnetic field strength observed by the DCMag instrument, with darker blues indicating smaller values. The black curves outline the statistical auroral oval. The gray thin curves depict the coastline. (b and c) Normalized integrated power (solid black curves) and normalized geomagnetic field strength (dashed gray curves) within the northern and southern auroral ovals, respectively, indicated by the black curves in panel a. The normalization ensures that corresponding maximum values are used as units. (d and e) Geographic distributions of the integrated power of the azimuthal and meridional components, respectively, of auroral magnetic fluctuations in the southern hemisphere. Circles represent latitudes (45°, 60° and 75°), while radial lines indicate longitudes (−90°, 0°, 90° and 180°) The black curves outline the statistical auroral oval.

19448007, 2024, 3, Downloaded from https://agupubs.onlinelibrary.wiley.com/doi/10.1029/2023GL107209 by Cochrane Iceland, Wiley Online Library on [27/01/2025]. See the Terms and Conditions (https://onlinelibrary.wiley.com/terms-and-conditions) on Wiley Online Library for rules of use; OA articles are governed by the applicable Creative Commons License

19448007, 2024, 3, Downloaded from https://agupubs.onlinelibrary.wiley.com/doi/10.1029/2023GL107209 by Cochrane Iceland, Wiley Online Library on [27/01/2025]. See the Terms and Conditions (https://onlinelibrary.wiley.com/terms-and-conditions) on Wiley Online Library for rules of use; OA articles are governed by the applicable Creative Commons License

We first examine the influence of seasons on P_B. For this purpose, we categorize P_B into two groups based on months: the winter-group (March, April, May, June, July, and August) and the summer-group (all other months). Geographic maps of P_B for the two groups are presented in Figures 3a and 3b, respectively. Evidently, both groups exhibit a notable decrease in P_B within the SAA longitude sector, resembling the pattern observed in Figure 2a. Additionally, it is worth noting that P_B in the summer-group appears slightly larger compared to that in the winter-group.

Next, we investigate P_B under different levels of geomagnetic activities. To represent the latter, we employ the SYM-H index and divide P_B into two groups accordingly: the quiet time-group (SYM-H > -20 nT) and the active time-group (SYM-H ≤ -20 nT). Geographic maps for both groups are presented in Figures 3c and 3d. In line with prior observations (e.g., Keiling et al., 2019; Liu et al., 2023), P_B during active times is larger than during quiet times. Nevertheless, the previously identified feature remains consistent across both groups: P_B within the SAA longitude sector is smaller than outside it.

All analyses above consider the SAA effect within the geographic space. However, generally speaking, the terrestrial aurora system, including auroral magnetic fluctuations, exhibits a more structured organization when viewed in the MLT-MLAT space, since it is primarily driven by the solar wind. Thus, we also examine the SAA effect within this framework for completeness. Figures 3e and 3f present the MLT-MLAT distributions of the P_B within the SAA longitude sector (from $-90°$ to $90°$ longitude) and outside of it, respectively. It is evident that P_B is smaller within the SAA longitude sector, across all MLT ranges covered. This observation indicates that the SAA effect is not confined to any specific MLT. Furthermore, these results also demonstrate that the decline in P_B at the SAA is not a result of any artificial effects arising from the mixing of different MLT sectors.

3. Auroral Intensity Observed by DMSP

The influence of the SAA is not restrict to auroral magnetic fluctuations but can also be observed in the aurora itself. To illustrate this, we show in Figures 4a and 4b the auroral intensity observed by the DMSP-17 satellite in the Lyman-Birge-Hopfield long (LBHL) band. This data set is precessed and analyzed in a similar manner to P_B shown Figure 2a. Particularly, we use the same MLT (i.e., nightside) and time interval for statistical analysis. Once again, we observe that the auroral intensity is weaker in the SAA longitude sector compared to other longitudes. It is worth noting that similar phenomena also appear on the dayside local time sector.

4. Discussion

The presented observations indicate that auroral magnetic fluctuations and auroral intensity are weaker in the SAA longitude sector compared to those outside of it. A comprehensive explanation for these observations would necessitate extensive numerical modeling, which is outside the scope of the present letter. Nevertheless, we offer some candidate mechanisms for consideration.

First, we discuss a potential geometry effect. Consider two regions of equal area within the southern auroral oval, with one in the SAA longitude sector and the other outside (denoted with subscripts "1" and "2" respectively). These two regions are connected to the equatorial plane by magnetic field lines, and the corresponding equatorial areas can be written as $A_1 = B_1/B_{e1}$ and $A_2 = B_2/B_{e2}$, respectively, where B_i and B_{ei} ($i = 1, 2$) represent the magnitude of the magnetic fields in the auroral oval areas and the corresponding equatorial areas, respectively. As a first-order approximation, we have $B_{e1} = B_{e2}$ since the magnetic fields far away from the Earth's surface are not significantly affected by magnetic anomalies. Thus, we observe $A_1/A_2 = B_1/B_2 < 1$, indicating that the auroral oval area within the SAA longitude sector is connected with a smaller equatorial area compared to those outside. Consequently, we would expect weaker auroral magnetic fluctuations and smaller auroral intensity within the SAA longitude sector if we assume they are associated with energy input from the equatorial plane.

Although the above scenario based on a pure geometry consideration can explain our observations, we do not rule out other explanations. For instance, it is reasonable to consider that the reduced B within the SAA affects the peak Alfvén speed along the corresponding magnetic field lines (located somewhere above the F-layer and also FY3E). This peak Alfvén speed plays a crucial role in the MIT coupling system as it acts as a partial reflecting boundary for waves. In simpler terms, when waves approach it from either the lower-altitude side or the higher-altitude side, they get reflected and cannot pass through to the opposite side. The significance of the

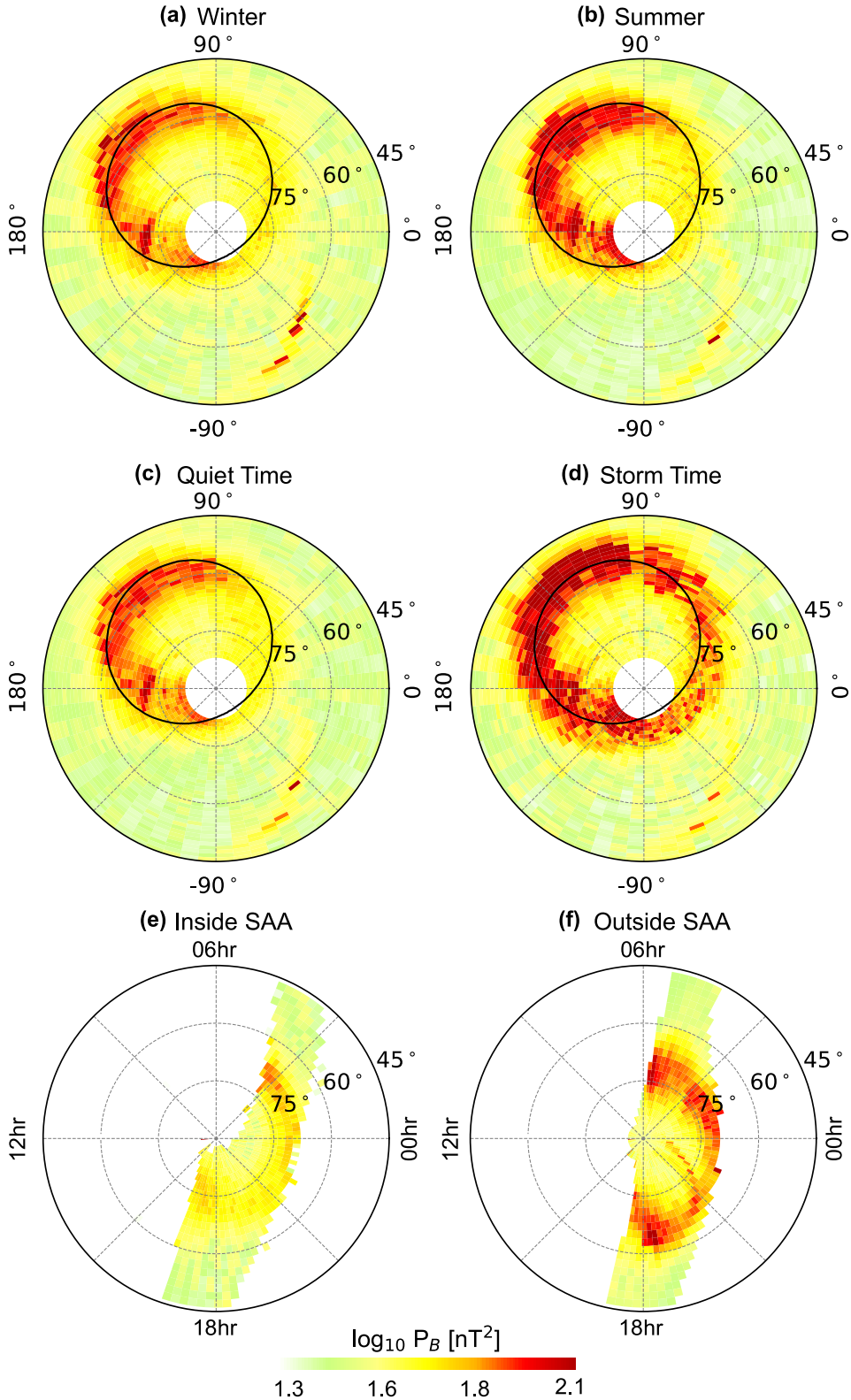

Figure 3.

19448007, 2024, 3, Downloaded from https://agupubs.onlinelibrary.wiley.com/doi/10.1029/2023GL107209 by Cochrane Iceland, Wiley Online Library on [27/01/2025]. See the Terms and Conditions (https://onlinelibrary.wiley.com/terms-and-conditions) on Wiley Online Library for rules of use; OA articles are governed by the applicable Creative Commons License

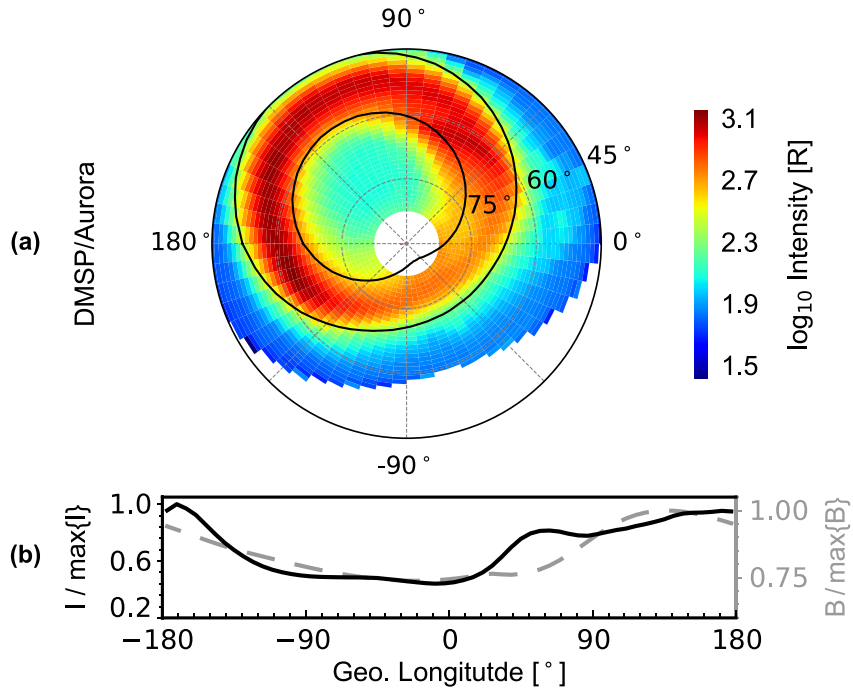

Figure 4. The auroral intensity in the LBHL band observed by the DMSP-17/SSUI instrument. (a) Geographic distributions of the auroral intensity, with the same format as Figures 3a–3d. (b) Normalized auroral intensity measured by the DMSP-17/SSUI instrument (solid black curves) and normalized geomagnetic field strength measured by the DCMag instrument (dashed gray curves) within the southern auroral oval indicated by the black curves in panel (a) The normalization ensures that corresponding maximum values are used as units.

peak Alfvén speed partially lies in its involvement in the formation of the ionospheric Alfvén resonator (IAR) (Poliakov & Rapoport, 1981; Lysak, 1993; Pokhotelov et al., 2001). The IAR represents a cavity bounded by the conducting E-layer and the peak Alfvén speed, capable of trapping waves within it. The smaller B values in the SAA longitude sector indicate a decrease in the peak Alfvén speed, leading to weaker wave reflection at the upper boundary of the IAR and consequently impairing the performance of the IAR. Hence, if we assume that most of the magnetic fluctuations observed in the auroral oval are related to the IAR, we would anticipate that they are weaker within the SAA longitude sector.

We acknowledge that the above arguments mostly remain hypotheses at present, and further studies are required to ascertain their validity. To comprehensively address this issue, a model that incorporates all the relevant components is necessary. We leave this for future studies.

While there is a need for further exploration of the underlying physics, our observations have already provided valuable insights into the magnetic field's impact on the terrestrial aurora and MIT coupling system. Previous studies (for example, see the review by Laundal et al., 2017] have predominantly focused on the north-south asymmetries in the magnetic field, revealing two principal factors: differences in field strength at conjugate points and the north-south asymmetries in the offset between the magnetic and geographic poles (e.g., Pakhotin et al., 2018). These findings suggest that the interplay between magnetically organized influences (e.g., the solar wind, interplanetary magnetic field and magnetospheric convection) and geographically organized forcing (e.g., sunlight) differs between the northern and southern hemispheres. On the other hand, our results indicate that, even when exclusively considering the southern hemisphere, the influence of the magnetic field is crucial. The inhomogeneity of the magnetic field strength by itself affects the aurora system independently of any interhemispheric

Figure 3. Geographic distributions of integrated power in auroral magnetic fluctuations in the southern hemisphere under different conditions: (a) winter months (March, April, May, June, July, and August), (b) summer months (September, October, November, December, January, and February), (c) quiet time (SYM-H index > -20 nT), and (d) active time (SYM-H index ≤ -20 nT). The format of these figures is similar to that of Figures 2d and 2e. (e and f) Magnetic local time-magnetic latitude distributions of integrated power in the southern hemisphere inside (between $-90°$ and $+90°$ longitudes) and outside (other longitudes) the South Atlantic Anomaly region corresponding, respectively. The format of these figures is similar to that of Figures 1f and 1g.

19448007, 2024, 3, Downloaded from https://agupubs.onlinelibrary.wiley.com/doi/10.1029/2023GL107209 by Cochrane Iceland, Wiley Online Library on [27/01/2025]. See the Terms and Conditions (https://onlinelibrary.wiley.com/terms-and-conditions) on Wiley Online Library for rules of use; OA articles are governed by the applicable Creative Commons License

19448007, 2024, 3, Downloaded from https://agupubs.onlinelibrary.wiley.com/doi/10.1029/2023GL107209 by Cochrane Iceland, Wiley Online Library on [27/01/2025]. See the Terms and Conditions (https://onlinelibrary.wiley.com/terms-and-conditions) on Wiley Online Library for rules of use; OA articles are governed by the applicable Creative Commons License

conjunction. Of course, this effect also introduces a north-south asymmetry, given that the magnetic fields exhibit greater inhomogeneity in the southern hemisphere compared to the northern hemisphere.

5. Summary

In summary, this work systematically investigates the magnetic fluctuations within the auroral oval observed by the AC Vector Magnetometer (ACMag) instrument onboard the Fengyun-3E satellite during 10 July 2021–24 April 2023. Unlike previous studies that primarily focused on local time or latitude dependence, this investigation centers on the geographic longitude dependence.

Data analysis reveals significant longitudinal variations in auroral magnetic fluctuations in the southern hemisphere. Specifically, these fluctuations are weaker in the longitude sector corresponding to the high-latitude part of the SAA compared to areas outside it. This characteristic remains constant throughout seasons and geomagnetic activity levels. Similar phenomena have been observed in the auroral intensity detected by the DMSP/SSUSI instruments. Hence, these observations demonstrate that the SAA substantially weakens the aurora system. In contrast, the auroral magnetic fluctuations and auroral intensity in the northern hemisphere remain relatively constant with respect to longitude, where the geomagnetic fields are homogenous as well.

The findings provide unambiguous evidence of the significant impact of the SAA on the aurora system. This result emphasizes the importance of considering the SAA in magnetospheric physics and presents an opportunity to examine the effects of non-dipole components of planetary magnetic fields (i.e., magnetic anomalies) on planetary magnetospheres and the magnetosphere-ionosphere-thermosphere coupling, including the FACs, aurora, magnetospheric precipitation and ionospheric outflows (Collin et al., 1998; Liu & Zong, 2022; Strangeway et al., 2005). In addition to its scientific implications, the study issues a caveat regarding research technique. It highlights the potential for misleading conclusions when simply combining all longitudes together to compare auroral dynamics in the southern hemisphere with those in the northern hemisphere, as usually done in previous studies (Knipp et al., 2021; Liu et al., 2023; Pakhotin et al., 2021).

Data Availability Statement

The DMSP/SSUSI data are archived at NASA's CDAWeb (https://spdf.gsfc.nasa.gov/pub/data/dmsp/dmspf17/ssusi/data/edr-aurora). The SYM-H index is archived at NASA's CDAWeb (https://cdaweb.gsfc.nasa.gov/pub/data/omni/omni_cdaweb/hro_1min/). The Fengyun-3E data are archived at Zenodo (Liu, 2023).

Acknowledgments
This work was supported by the National Natural Science Foundation of China 42230202 (Q.G.Z), the Major Project of Chinese National Programs for Fundamental Research and Development 2021YFA0718600 (Q.G.Z.), the China Space Agency project D020301 (Q.G.Z), the Science and Technology Development Fund, Macau SAR (File no. SKL-LPS(MUST)-2024-2026), and the China National Postdoctoral Program for Innovative Talents BX20230030 (Z.Y.L.). We thank the Peking University instrument development team for providing the FY-3E/ACMag and FY-3E/DCMag data. We are also grateful to the DMSP/SSUSI team for providing the aurora data.

References

Badhwar, G. D. (1997). Drift rate of the south atlantic anomaly. *Journal of Geophysical Research*, *102*(A2), 2343–2349.

Billett, D. D., McWilliams, K. A., Pakhotin, I. P., Burchill, J. K., Knudsen, D. J., & Martin, C. J. (2022). High-resolution poynting flux statistics from the swarm mission: How much is being underestimated at larger scales? *Journal of Geophysical Research: Space Physics*, *127*(7), e2022JA030,573. https://doi.org/10.1029/2022ja030573

Collin, H., Peterson, W., Lennartsson, O., & Drake, J. (1998). The seasonal variation of auroral ion beams. *Geophysical Research Letters*, *25*(21), 4071–4074. https://doi.org/10.1029/1998gl900090

Connerney, J., Acuña, M., Wasilewski, P., Kletetschka, G., Ness, N., Reme, H., et al. (2001). The global magnetic field of mars and implications for crustal evolution. *Geophysical Research Letters*, *28*(21), 4015–4018. https://doi.org/10.1029/2001gl013619

Connerney, J., Timmins, S., Oliversen, R., Espley, J., Joergensen, J., Kotsiaros, S., et al. (2022). A new model of Jupiter's magnetic field at the completion of Juno's prime mission. *Journal of Geophysical Research: Planets*, *127*(2), e2021JE007,055. https://doi.org/10.1029/2021je007055

Consolini, G., De Michelis, P., Alberti, T., Giannattasio, F., Coco, I., Tozzi, R., & Chang, T. (2020). On the multifractal features of low-frequency magnetic field fluctuations in the field-aligned current ionospheric polar regions: Swarm observations. *Journal of Geophysical Research: Space Physics*, *125*(5), e2019JA027,429. https://doi.org/10.1029/2019ja027429

Erlandson, R., & Zanetti, L. (1998). A statistical study of auroral electromagnetic ion cyclotron waves. *Journal of Geophysical Research*, *103*(A3), 4627–4636. https://doi.org/10.1029/97ja03169

Finlay, C. C., Kloss, C., Olsen, N., Hammer, M. D., Tøffner-Clausen, L., Grayver, A., & Kuvshinov, A. (2020). The chaos-7 geomagnetic field model and observed changes in the south Atlantic anomaly. *Earth Planets and Space*, *72*(1), 1–31. https://doi.org/10.1186/s40623-020-01252-9

Ginet, G., O'Brien, T., Huston, S., Johnston, W., Guild, T., Friedel, R., et al. (2014). *Ae9, ap9 and SPM: New models for specifying the trapped energetic particle and space plasma environment* (pp. 579–615). The Van Allen Probes Mission.

Gledhill, J. (1976). Aeronomic effects of the south Atlantic anomaly. *Reviews of Geophysics*, *14*(2), 173–187. https://doi.org/10.1029/rg014i002p00173

Golovchanskaya, I., Ostapenko, A., & Kozelov, B. (2006). Relationship between the high-latitude electric and magnetic turbulence and the birkeland field-aligned currents. *Journal of Geophysical Research*, *111*(A12). https://doi.org/10.1029/2006ja011835

Grodent, D., Bonfond, B., Gérard, J.-C., Radioti, A., Gustin, J., Clarke, J. T., et al. (2008). Auroral evidence of a localized magnetic anomaly in Jupiter's northern hemisphere. *Journal of Geophysical Research*, *113*(A9). https://doi.org/10.1029/2008ja013185

Heirtzler, J. R. (2002). The future of the south Atlantic anomaly and implications for radiation damage in space. *Journal of Atmospheric and Solar-Terrestrial Physics*, *64*(16), 1701–1708. https://doi.org/10.1016/s1364-6826(02)00120-7

Hu, Z.-J., Yang, Q.-J., Liang, J.-M., Hu, H.-Q., Zhang, B.-C., & Yang, H.-G. (2017). Variation and modeling of ultraviolet auroral oval boundaries associated with interplanetary and geomagnetic parameters. *Space Weather*, *15*(4), 606–622. https://doi.org/10.1002/2016sw001530

Iijima, T., & Potemra, T. A. (1978). Large-scale characteristics of field-aligned currents associated with substorms. *Journal of Geophysical Research*, *83*(A2), 599–615. https://doi.org/10.1029/ja083ia02p00599

Keiling, A., Thaller, S., Wygant, J., & Dombeck, J. (2019). Assessing the global Alfvén wave power flow into and out of the auroral acceleration region during geomagnetic storms. *Science Advances*, *5*(6), eaav8411. https://doi.org/10.1126/sciadv.aav8411

Keiling, A., Wygant, J., Cattell, C., Mozer, F., & Russell, C. (2003). The global morphology of wave poynting flux: Powering the aurora. *Science*, *299*(5605), 383–386. https://doi.org/10.1126/science.1080073

Knipp, D., Kilcommons, L., Hairston, M., & Coley, W. R. (2021). Hemispheric asymmetries in poynting flux derived from DMSP spacecraft. *Geophysical Research Letters*, *48*(17), e2021GL094,781. https://doi.org/10.1029/2021gl094781

Langlais, B., Purucker, M., & Mandea, M. (2004). Crustal magnetic field of mars. *Journal of Geophysical Research*, *109*(E2). https://doi.org/10.1029/2003je002048

Laundal, K. M., Cnossen, I., Milan, S. E., Haaland, S., Coxon, J., Pedatella, N., et al. (2017). North–south asymmetries in earth's magnetic field: Effects on high-latitude geospace. *Space Science Reviews*, *206*(1–4), 225–257. https://doi.org/10.1007/s11214-016-0273-0

Liu, Z.-Y. (2023). Dataset for "the impact of the south Atlantic anomaly on the aurora system" [Dataset]. Zenodo. https://doi.org/10.5281/zenodo.10394208

Liu, Z.-Y., & Zong, Q.-G. (2022). Ionospheric oxygen outflows directly injected into the inner magnetosphere: Van Allen probes statistics. *Journal of Geophysical Research: Space Physics*, *127*(10), e2022JA030,611. https://doi.org/10.1029/2022ja030611

Liu, Z.-Y., Zong, W.-G., Zong, Q.-G., Wang, J.-S., Yu, X.-Q., Wang, Y.-F., et al. (2023). The response of auroral-oval waves to cir-driven recurrent storms: Fy-3e/acmag observations. *Universe*, *9*(5), 213. https://doi.org/10.3390/universe9050213

Lühr, H., Park, J., Gjerloev, J. W., Rauberg, J., Michaelis, I., Merayo, J. M., & Brauer, P. (2015). Field-aligned currents' scale analysis performed with the swarm constellation. *Geophysical Research Letters*, *42*(1), 1–8. https://doi.org/10.1002/2014gl062453

Lysak, R. L. (1993). *Generalized model of the ionospheric Alfvén resonator* (Vol. 80, pp. 121–128). Washington DC American Geophysical Union Geophysical Monograph Series.

Pakhotin, I., Mann, I., Knudsen, D., Lysak, R., & Burchill, J. (2020). Diagnosing the role of Alfvén waves in global field-aligned current system dynamics during southward IMF: Swarm observations. *Journal of Geophysical Research: Space Physics*, *125*(1), e2019JA027,277. https://doi.org/10.1029/2019ja027277

Pakhotin, I., Mann, I., Lysak, R., Knudsen, D., Gjerloev, J., Rae, I., et al. (2018). Diagnosing the role of Alfvén waves in magnetosphere-ionosphere coupling: Swarm observations of large amplitude nonstationary magnetic perturbations during an interval of northward IMF. *Journal of Geophysical Research: Space Physics*, *123*(1), 326–340. https://doi.org/10.1002/2017ja024713

Pakhotin, I., Mann, I., Xie, K., Burchill, J., & Knudsen, D. (2021). Northern preference for terrestrial electromagnetic energy input from space weather. *Nature Communications*, *12*(1), 199. https://doi.org/10.1038/s41467-020-20450-3

Paschmann, G., Haaland, S., Treumann, R., & Treumann, R. A. (2003). *Auroral plasma physics* (Vol. 15). Springer Science & Business Media.

Paxton, L. J., & Meng, C.-I. (1999). Auroral imaging and space-based optical remote sensing. *Johns Hopkins APL Technical Digest*, *20*(4), 556–569.

Paxton, L. J., Morrison, D., Zhang, Y., Kil, H., Wolven, B., Ogorzalek, B. S., et al. (2002). Validation of remote sensing products produced by the special sensor ultraviolet scanning imager (SSUSI): A far UV-imaging spectrograph on DMSP f-16. In *Optical spectroscopic techniques, remote sensing, and instrumentation for atmospheric and space research IV* (Vol. 4485, pp. 338–348). SPIE.

Pokhotelov, O. A., Khruschev, V., Parrot, M., Senchenkov, S., & Pavlenko, V. (2001). Ionospheric Alfvén resonator revisited: Feedback instability. *Journal of Geophysical Research*, *106*(A11), 25813–25824. https://doi.org/10.1029/2000ja000450

Poliakov, S., & Rapoport, V. (1981). The ionospheric Alfvén resonator. *Geomagnetism and Aeronomy*, *21*, 816–822.

Roederer, J. G., & Zhang, H. (2016). *Dynamics of magnetically trapped particles*. Springer.

Shepherd, S. (2014). Altitude-adjusted corrected geomagnetic coordinates: Definition and functional approximations. *Journal of Geophysical Research: Space Physics*, *119*(9), 7501–7521. https://doi.org/10.1002/2014ja020264

Strangeway, R., Ergun, R., Su, Y.-J., Carlson, C., & Elphic, R. (2005). Factors controlling ionospheric outflows as observed at intermediate altitudes. *Journal of Geophysical Research*, *110*(A3). https://doi.org/10.1029/2004ja010829

Trenchi, L., Team, F.-M., Kauristie, K., Käki, S., Vanhamäki, H., Juusola, L., et al. (2020). ESA field-aligned currents methodology inter-comparison exercise. In *Ionospheric multi-spacecraft analysis tools: Approaches for deriving ionospheric parameters* (pp. 167–188).

Underwood, C. I. (2003). Observations of radiation in the space radiation environment and its effect on commercial off-the-shelf electronics in low-earth orbit. *Philosophical Transactions of the Royal Society of London,Series A: Mathematical, Physical and Engineering Sciences*, *361*(1802), 193–197. https://doi.org/10.1098/rsta.2002.1122

Yu, X.-Q., Huang, C., Xiao, C.-J., Li, J.-W., Liu, S., Wang, J.-D., et al. (2023). Ac vector magnetometer for space-based applications using low-resource magneto-impedance sensor. *Science China Technological Sciences*, *66*(12), 3663–3670. https://doi.org/10.1007/s11431-022-2390-2

Yu, X.-Q., Li, J.-W., Xiao, C.-J., Huang, C., Liu, S., Wang, J.-D., et al. (2023). Vector magnetometer for space applications based on a low-resource magnetoresistance. *Acta Scientiarum Naturalium Universitatis Pekinensis*.

19448007, 2024, 3, Downloaded from https://agupubs.onlinelibrary.wiley.com/doi/10.1029/2023GL107209 by Cochrane Iceland, Wiley Online Library on [27/01/2025]. See the Terms and Conditions (https://onlinelibrary.wiley.com/terms-and-conditions) on Wiley Online Library for rules of use; OA articles are governed by the applicable Creative Commons License